L.-W. Hung and C. T.-C. Nguyen, "Capacitive-piezo transducers for higher *Q* contour-mode AlN resonators at 1.2 GHz," *Tech. Digest*, 2008 Solid-State Sensor, Actuator, and Microsystems Workshop, Hilton Head, South Carolina, June 6-10, 2010, pp. 463-466.

CAPACITIVE-PIEZO TRANSDUCERS FOR HIGHER *Q* CONTOUR-MODE ALN RESONATORS AT 1.2GHZ

Li-Wen Hung and Clark T.-C. Nguyen
Department of Electrical Engineering and Computer Science
University of California at Berkeley, Berkeley, CA 94720-1774, U.S.A.

ABSTRACT

A "capacitive-piezo" transducer that combines the strengths of capacitive and piezoelectric mechanisms to achieve an impedance and *Q* simultaneously lower and higher, respectively, than otherwise attainable by either mechanism separately, has allowed demonstration of a 1.2-GHz contour-mode AlN ring resonator with a motional resistance of 889 Ω and *Q*=3,073 higher than so far measured for any other d_{31}-transduced piezoelectric resonator at this frequency. Here, the key innovation is to separate the piezoelectric resonator from its metal electrodes by tiny gaps to eliminate metal material and metal-to-piezoelectric interface losses thought to limit thin-film piezoelectric resonator *Q*'s, while also maintaining high electric field strength to preserve a strong piezoelectric effect. In addition, this capacitive-piezo transducer concept does not require dc-bias voltages and allows for much thicker electrodes that then lower series resistance without mass loading the resonant structure. The latter is especially important as resonators and their supports continue to scale towards even higher frequencies.

INTRODUCTION

The ever-increasing appetite for wireless interconnectivity is beginning to drive new functions, like frequency gating spectrum analysis [1], that in turn drive a need for GHz resonators with simultaneous high *Q* (>30,000) and low impedance (<200 Ω). Unfortunately, no single on-chip resonator device can deliver such performance in this frequency range. Indeed, among popular resonator choices, thin-film piezoelectric (e.g., AlN) resonators post lower electrical impedances, but also lower mechanical *Q*'s (e.g., R_x=125 Ω and *Q*=2,100 [2]), than capacitive counterparts (e.g., R_x=12.8 kΩ and *Q*=48,048 [3]) at comparable (~60 MHz) frequencies. To achieve simultaneous high *Q* and low impedance, either the impedance of capacitive resonators must be lowered [4][5], or the *Q*'s of piezoelectric resonators must be raised.

This work focuses on the latter and specifically introduces a new "capacitive-piezo" transducer, shown in Fig.1(b), that combines the strengths of capacitive and piezoelectric mechanisms to achieve an impedance and *Q* simultaneously lower and higher, respectively, than otherwise attainable by either mechanism separately. Using this new transducer, a 1.2-GHz contour-mode AlN ring resonator achieves a motional resistance of 889 Ω and a *Q*=3,073 higher than so far measured for any other d_{31}-transduced piezoelectric resonator at this frequency. The key innovation here is to separate the piezoelectric resonator from its metal electrodes by tiny gaps to eliminate metal material and metal-to-piezoelectric interface losses thought to limit thin-film piezoelectric resonator *Q*'s, while also maintaining high electric field strength to preserve a strong piezoelectric effect. To understand the logic behind this approach, the next section starts off with some discussion of previous attempts to raise piezoelectric resonator *Q*'s.

RAISING PIEZOELECTRIC RESONATOR *Q*

Indeed, plenty of researchers have sought to raise the *Q*'s of thin-film piezoelectric resonators, with approaches that span from reducing electrode roughness [6], to optimizing the electrode material [7], to carefully balancing the AlN-to-electrode thickness ratio [8], to use of a Bragg reflector to prevent energy loss [9]. Unfortunately, none of the above methods raises the *Q*'s of on-chip piezoelectric resonators anywhere near the >30,000 values needed for RF channel-selection and frequency gating spectrum analyzers.

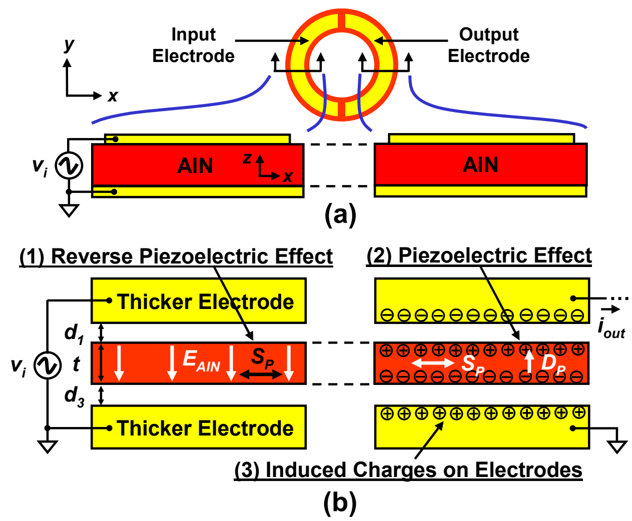

Fig.1: (a) Conventional piezoelectric transducers employing electrodes that directly contact the piezoelectric structure; and (b) working principals behind a capacitive-piezo resonator for which electrodes are separated from the piezoelectric structure via tiny air gaps.

Yet, polysilicon resonators easily achieve such *Q* values (but with higher than-desired impedances). To date, the measured *Q*'s of polysilicon resonators are on the order of 20 times larger than that of sputtered AlN resonators at similar frequencies. Interestingly, material loss theory [10][11][12] predicts that the ($f{\cdot}Q$) product limit due to (dominant) phonon-phonon interactions in the AlN material itself is only four times lower than that of silicon. This suggests that the AlN material itself might not be the principal culprit among *Q*-limiting losses, but rather the metal electrodes or the electrode-to-resonator interface strain might be more responsible. In fact, experimental data shows that as the thickness of a piezoelectric resonator's electrode increases, both the resonance frequency and *Q* of the resonator drop due to mass loading and electrode loss, respectively [13]. Electrode-derived energy loss perhaps also contributes to the lower *Q*'s measured in d_{31}-transduced resonators, where the electrodes often cover locations with the maximum strain, versus the *Q*'s of d_{33}-transduced thickness-mode resonators, where electrodes are placed very close to the nodes of the acoustic standing waves. Of course, despite their lower *Q*'s, d_{31}-transduced resonators are arguably more attractive than d_{33}, since their frequencies are set by CAD-definable lateral dimensions, so are more suitable for on-chip integration of multiple frequencies.

Whether a resonator uses d_{31} or d_{33}, both share the common problem that *Q* gets worse as dimensions scale to achieve larger coupling and/or higher frequencies. In particular, while a piezoelectric structure can be scaled, its electrode thickness often cannot scale as aggressively, since doing so incurs excessive electrical loss derived from increased electrode and interconnect electrical resistance. If a designer attempts to compensate for this by using thinner, but wider, metal traces, then the beams supporting the resonator would need to be wider to accommodate the wider metal traces, and wider beams incur more energy loss through supports

L.-W. Hung and C. T.-C. Nguyen, "Capacitive-piezo transducers for higher Q contour-mode AlN resonators at 1.2 GHz," *Tech. Digest*, 2008 Solid-State Sensor, Actuator, and Microsystems Workshop, Hilton Head, South Carolina, June 6-10, 2010, pp. 463-466.

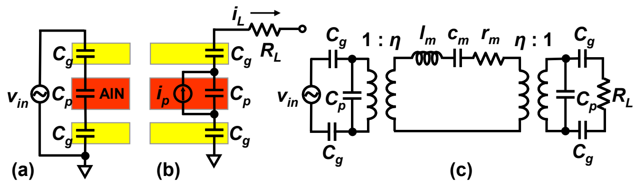

Fig. 2: Equivalent electrical circuit at (a) input and (b) output, modeling the effect of gap spacing on the electromechanical coupling coefficient; (c) equivalent circuit of a capacitive-piezo resonator. Here, η is the coupling coefficient with gap spacing d_{Total}=0.

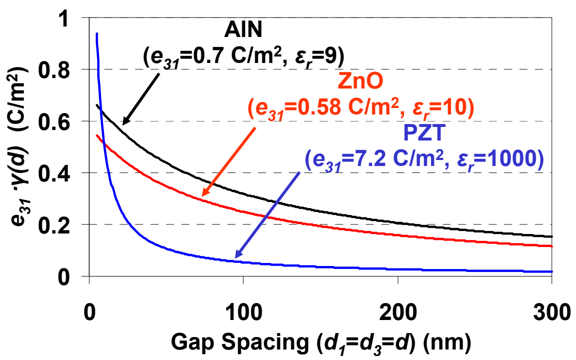

Fig. 3: The effective e_{31} on the drive side decreases as the gap spacing increases. The gap spacing affects the coupling of PZT the most due to its much larger relative permittivity ε_r.

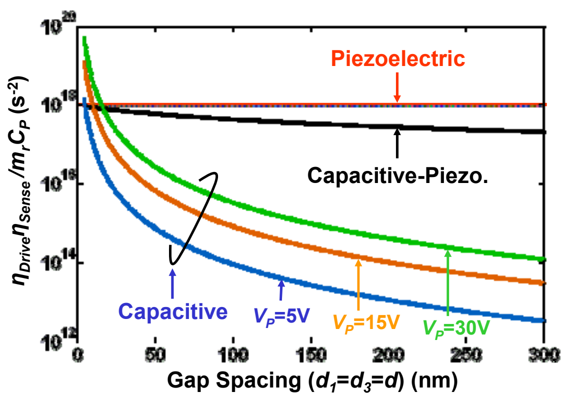

Fig. 4: Comparison of filter FOM of different transducers as a function of gap spacing, given the same filter bandwidth and type.

and anchors, hence lower Q. If the width of the support beams are decreased in order to lower anchor losses and raise Q, the width of the metal traces must also be decreased, which then increases their resistance, again, lowering Q and negating the gains.

CAPACITIVE-PIEZO TRANSDUCERS

From the above discussion, it seems that Q degradation cannot be avoided as long as the electrode is in physical contact with the piezoelectric structure (which generates loss through strain coupling) and as long as the piezoelectric structure governs the size and thickness of the electrode (which governs electrical loss). Interestingly, all of these issues can be circumvented by mechanically decoupling the electrodes from the resonating body by simply separating the electrodes from the vibrating structure so that they are no longer in contact, as shown in Fig.1(b). The resulting transducer, dubbed the "capacitive-piezo" transducer, should not only raise the Q of the piezoelectric film, but should also allow much thicker (and thus much less resistive) electrodes without the electrode loss and mass loading penalties that would otherwise result if the electrode is contacted as in Fig.1(a). Thicker electrodes should also further increase the Q, since the electrode parasitic series resistance would be smaller.

Although not a well known technique, the use of contactless electrodes on piezoelectric resonators is actually not new. This strategy had in fact been demonstrated on 5- and 10-MHz quartz crystal resonators, called BVA resonators, as far back as 1977 [14]. Since the piezoelectric-to-electrode thickness ratio of these devices was on the order of 100µm-to-100nm, or 1000, separating the electrode from the piezoelectric did little to increase the Q of the device. It did, however, allow for a more stable device against drift, since it eliminates electrode-to-resonator stress variations. This was the main reason for investigating such devices in the past.

For micromechanical resonators, on the other hand, the piezoelectric-to-electrode thickness ratio is much smaller, on the order of 10. Thus, the case for using a "capacitive-piezo" transducer is much stronger on the micro-scale. In addition, the ease with which tiny electrode-to-resonator gaps can be achieved via MEMS technologies further encourages the use of contactless electrodes. In effect, capacitive-piezo transducers stand to improve the Q and drift stability of micro-scale thin-film piezoelectric resonators with very little increase in fabrication cost.

ANALYTICAL MODELING

Electrical models for AlN contour-mode resonators with contacting electrodes, such as described in [1], are abundant in the literature. The present approach to modeling the capacitive-piezo resonator focuses on how electrode-to-resonator air gaps influence the electrical model parameters. Pursuant to this, Fig.1(b) presents the cross-section of a contour-mode resonator with capacitive-piezo transducers under a typical excitation configuration. When the input signal is applied across the top and bottom electrodes, mechanical strain, S_P, is induced on the AlN film via the reverse piezoelectric effect. The induced strain is linearly proportional to both the piezoelectric stress constant, e_{31} (e_{31}~0.7 C/m^2 for sputtered AlN), and the electric field established within the AlN film, E_{AlN}, regardless of the mode shape of the resonator. The gap-AlN-gap stack can be modeled by three capacitors in series, as shown in Fig. 2(a), from which E_{AlN} can be written as

$$E_{AlN} = \frac{v_{in}}{t + \varepsilon_r d_{Total}} \qquad (1)$$

where ε_r (~9) and t are the relative permittivity in the c-axis direction and thickness of AlN, respectively; and d_{Total} is the total gap spacing (d_{Total}=d_1+d_3). When the input frequency matches the resonance frequency, the lateral force F_P induced by E_{AlN} via the reverse piezoelectric effect excites the resonator into lateral-mode vibration with an electromechanical coupling coefficient on the drive side given by

$$\eta_{Drive} = \frac{F_P}{v_{in}} = \alpha \cdot e_{31} \cdot \frac{t}{t + \varepsilon_r d_{Total}} = \alpha \cdot e_{31} \cdot \gamma(d_{Total}) \qquad (2)$$

where the value of α depends on the electrode coverage area and placement, and on the resonator mode shape; and where $\gamma(d_{Total})$ is a function gauging how much the coupling coefficient degrades with increasing air gap spacing. Fig. 3 plots the ($e_{31} \cdot \gamma(d_{Total})$) product for different piezoelectric materials. In general, small gap spacing is preferred to maintain a high coupling coefficient. It should be noted that a large e_{31} does not guarantee a large coupling coefficient. As shown in Fig. 3, even though PZT has a larger e_{31} than AlN and ZnO, its capacitive-piezo coupling is weaker at most gap spacings due to its much higher relative permittivity.

On the sense side, vibration-induced strain polarizes the AlN film via the piezoelectric effect, and the resulting electric displacement can be expressed as

L.-W. Hung and C. T.-C. Nguyen, "Capacitive-piezo transducers for higher *Q* contour-mode AlN resonators at 1.2 GHz," *Tech. Digest*, 2008 Solid-State Sensor, Actuator, and Microsystems Workshop, Hilton Head, South Carolina, June 6-10, 2010, pp. 463-466.

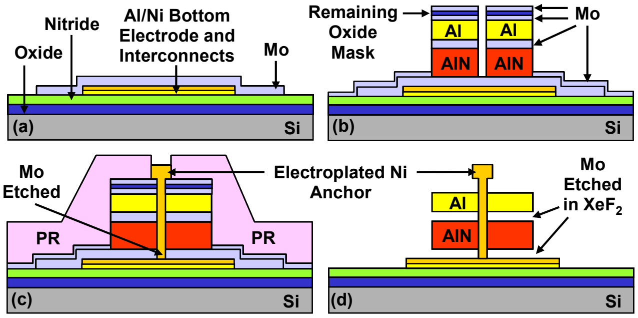

Fig. 5: Fabrication process flow of capacitive-piezo AlN resonator with electroplated Ni anchor and Mo sacrificial material dry released in XeF_2.

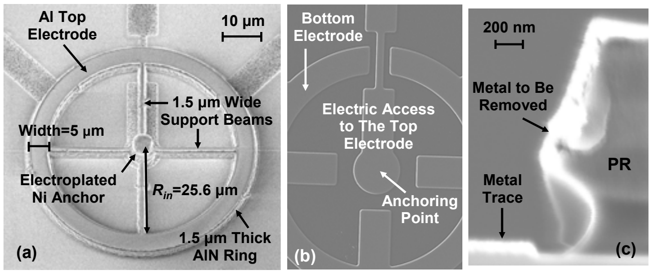

Fig. 6: (a) Fabricated 1.2-GHz capacitive-piezo AlN ring resonator; (b) bottom electrode and interconnect configuration, showing anchoring at the very center; (c) cross sectional SEM showing the double-layer lift-off process that ensures smooth metal trace edges.

$$D_P = e_{31}S_P = e_{31}\left[\frac{\partial u_x}{\partial x}+\frac{\partial u_y}{\partial y}\right] \quad (3)$$

where u_x and u_y are the mechanical displacements in the *x* and *y* directions, respectively. Assuming a perfectly aligned AlN film and no spurious modes, AlN is uniformly polarized (i.e., with only bound surface charges and no bound body charges), D_P is purely along the vertical direction, and the integral of D_P over the entire electrode area equates to the total amount of induced charge Q_P, the time derivative of which becomes the current i_P. The piezoelectric effect on the sense side can thus be modeled by a current source with magnitude $i_P=\omega\cdot Q_P$ as shown in Fig. 2(b), and the output current, i.e., the current flowing though R_L (R_L =50 Ω for measurement with a network analyzer), becomes

$$i_{Out} = i_P\cdot\frac{Z_P}{Z_P+Z_g+Z_g+R_L} \approx i_P\cdot\frac{t}{t+\varepsilon_r d_{Total}} = i_P\cdot\gamma \quad (4)$$

From (4), the electromechanical coupling coefficient on the sense side, η_{Sense}, is also a function of the gap spacing through $\gamma(d_{Total})$. Although air gaps degrade k_t^2 by a factor of γ^2, the higher *Q* provided by non-contacting electrodes together with sufficiently small gap spacings actually make it possible to achieve higher $Q\cdot k_t^2$ than piezoelectric resonators with contacting electrodes.

Perhaps the best way to compare different transducers is via the filter *FOM* defined in [4], given by

$$FOM = \frac{1}{R_Q C_o} \propto \frac{\eta_{Drive}\eta_{Sense}}{m_r C_o} \quad (5)$$

where R_Q is the filter termination resistor, C_o the physical input capacitance, and m_r the motional mass of a constituent resonator in the filter. The right most form delineates parameters in the expanded equation most relevant to resonator design.

Fig. 4 compares simulated plots of ($\eta_{Drive}\eta_{Sense}/m_rC_o$) in the filter *FOM* for three different transducers (i.e. piezoelectric, capacitive-piezo, and capacitive alone) versus gap spacing *d* ($d=d_1=d_3$) at the same frequency. The simulation uses a ring inner radius and thickness of 25.6 µm and 1.5 µm, respectively; and ring widths of

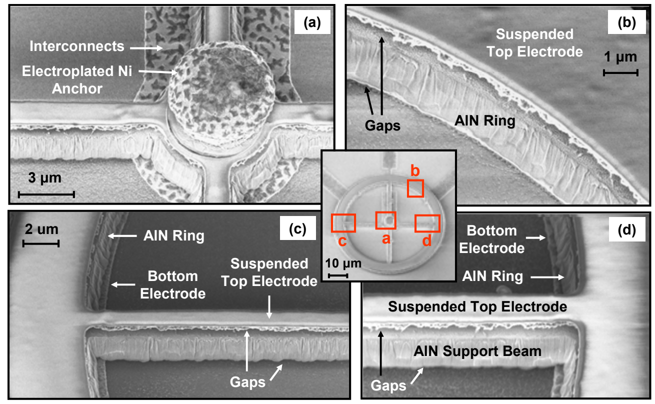

Fig. 7: SEM's at different parts of the same resonator confirming that the entire top electrode and the AlN ring resonator are suspended via the electroplated nickel anchor at the center.

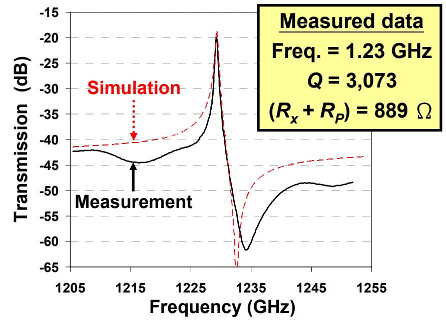

Simulation Parameters	
Young's Modulus	350 GPa
Density	3230 kg/m³
ε_{AlN}	9
e_{31}	0.7 C/m²
Q	3,073
r_m	43.8 Ω
l_m	1.86x10⁻¹² H
c_m	9.08x10⁻⁹ F
η	3.26x10⁻⁴
C_{Gap}	2.61x10⁻¹⁴ F
C_P	4.07x10⁻¹⁴ F

Fig. 8: Measured frequency characteristic for a 1.2-GHz AlN ring resonator with dimensions as shown in Fig. 6 and equivalent circuit of Fig. 2(c).

5 µm for AlN and 4.3 µm for polysilicon, both chosen to achieve a 1.2-GHz resonance frequency for both materials under the same mode shape, neglecting DC bias-induced electrical spring softening inherent to capacitive resonators. In addition, the electrodes for the polysilicon resonator are assumed to be placed both inside and outside the ring, similar to [3]. As expected, the *FOM* of the capacitive-piezo transducer depends on gap spacing, but not as strongly as one might think, mainly because C_o drops by the same ratio γ as the electromechanical coupling coefficient when the gap spacing increases. Even so, a capacitive-piezo transducer with a 200 nm gap spacing achieves ($\eta_{Drive}\eta_{Sense}/m_rC_o$) of 2.7×10^{17} s^{-2}, for which a capacitive (alone) transducer would require a much smaller gap spacing of 23 nm. Needles to say, this relaxed gap spacing is a distinct advantage of capacitive-piezo transducers over capacitive.

FABRICATION

AlN resonators employing capacitive-piezo transducers were fabricated using a newly-developed 4-mask low-temperature CMOS-compatible process briefly summarized in Fig. 5. Here, aluminum top and Al/Ni bottom electrodes are temporarily separated from the AlN structure by a sputtered molybdenum (Mo) sacrificial material. Molybdenum is used as a sacrificial material instead of the oxide, silicon, or germanium, more commonly used in surface-micromachining processes, mainly to attain better c-axis orientation when sputtering the AlN film. Anchoring for all suspended structures, including the AlN and top electrode, is realized by a single electroplated nickel peg that contacts the top electrode. The device is released via a gaseous XeF_2/N_2 etchant.

Fig. 6(a) presents the wide-view SEM of a completed 1.2-GHz contour-mode d_{31}-capacitive-piezo-transduced ring resonator. Fig. 7 presents SEM's of different parts of the same ring resonator delineating the gaps between the top/bottom electrode and the

L.-W. Hung and C. T.-C. Nguyen, “Capacitive-piezo transducers for higher *Q* contour-mode AlN resonators at 1.2 GHz,” *Tech. Digest*, 2008 Solid-State Sensor, Actuator, and Microsystems Workshop, Hilton Head, South Carolina, June 6-10, 2010, pp. 463-466.

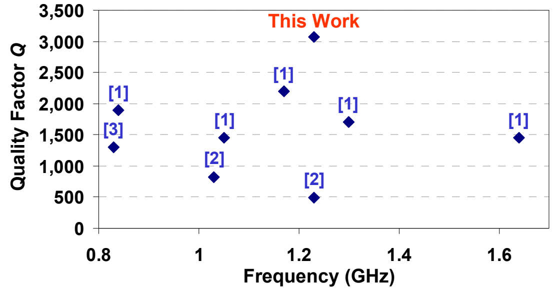

Fig. 9: Comparison of Q's achieved via the capacitive-piezo AlN ring resonator of this work versus other ~1 GHz lateral-mode AlN resonators.

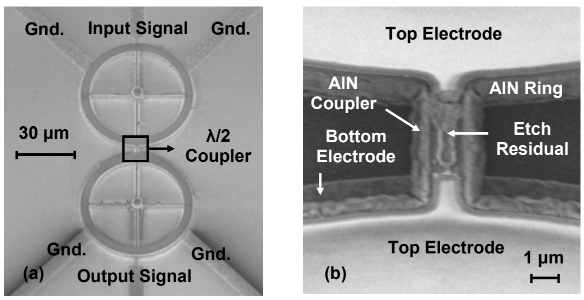

Fig. 10: (a) SEM of a capacitive-piezo ring resonator array with λ/2 coupler; and (b) top-view SEMS showing how the electrode is removed from the coupler to electrically isolate the output from the input.

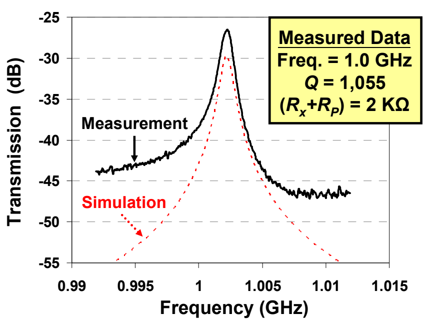

Simulation Parameters

Young's Modulus	350 GPa
Density	3230 kg/m³
ε_{AlN}	9
e_{31}	0.7 C/m²
Q	1,055
r_m	127 Ω
l_m	3.72x10^{-12} H
c_m	4.54x10^{-9} F
η	3.26x10^{-4}
C_{Gap}	2.61x10^{-14} F
C_P	4.07x10^{-14} F

Fig. 11: Measured frequency characteristic for the resonator of Fig. 10, confirming suppression of the parallel resonance peak.

resonator. For this device, to reduce electrode resistance, 400 nm thick Al is used as the top electrode—something that otherwise would not be permissible in a conventional AlN resonator, since its attached electrode would mass load the resonant structure.

MEASUREMENTS

Fig. 8 presents the measured frequency response characteristics for the AlN ring resonator of Fig. 6(a), showing f_s=1.23 GHz, Q=3,073, and R_x=889 Ω at 3 mTorr. Both the input and output are DC grounded via bias-tee's to avoid electrostatic forces that might pull the top and bottom electrodes together and into the AlN resonator. Although the measured Q is still less than predicted by material loss theory, it is still substantially higher than any other measured contour-mode AlN resonator at similar frequencies, as plotted in Fig. 9 [15][16][17]. The etch residuals observed in the gaps after release, as shown in Fig. 7, may have affected the measured Q. Moreover, it has been confirmed experimentally that electroplated Ni anchors are mechanically weaker and more poorly attached to the substrate than the PECVD polysilicon anchors used in previous capacitive resonators. This may induce more anchor loss, especially at high frequencies. Finally, due to process difficulties, the supports of the final fabricated resonators deviated from quarter-wavelength dimensions, and this further lowers Q.

It should be noted that the 260 nm gap spacing used in this device is a rather conservative design. In fact, if the gap spacing were reduced from 260 nm to the 100 nm commonly used in capacitive (only) resonators, the impedance could be lowered to 250 Ω.

To evaluate the efficacy of building mechanical circuits using capacitive-piezo transducers, mechanically coupled two-resonator arrays, shown in Fig. 10, were also fabricated and tested. Here, the top electrode on the coupling beam is removed to electrically isolate the output from the input. The measured frequency response, shown in Fig. 11, exhibits much less feedthrough than seen in single-electrode devices. However, the Q is lower for this mechanical circuit than for a single resonator, which might be caused by etch residuals atop the coupling beam formed after dry etching the top electrode. Fixes to this problem are underway.

CONCLUSIONS

This paper demonstrated a 1.2-GHz contour-mode AlN ring resonator with a motional resistance of 889 Ω and Q=3,073, confirming that resonators equipped with “capacitive-piezo” transducers can achieve higher Q than so far measured for any other d_{31}-transduced piezoelectric resonator at this frequency and at the same time maintain high electromechanical coupling. Although the demonstrated Q is higher than other piezoelectric resonators, it is probably far from what is achievable using this technology. In particular, it is not unreasonable to expect that future capacitive-piezo equipped resonators with better defined quarter-wave length supports and stiffer anchors might eventually achieve the Q's in the tens of thousands predicted by the theory.

ACKNOWLEDGEMENTS*:* This work is supported by DARPA. The authors would like to thank Berkeley Microlab staff and members, especially Dr. X. Meng, Dr. J. Black, Dr. P. Stephanou, and J. Donnelly, for their assistance and advice on fabrication.

REFERENCES

[1] C. T.-C. Nguyen, "Integrated micromechanical RF…," *26th Sym. on Sensors, Micromachines, and App. Sys*., pp. 1-5, 2009.
[2] G. Piazza, *et. al*., “Piezoelectric aluminum nitride…,” *J. IEEE/ASME Microelectromech. Syst*, vol. 15, pp. 1406-1418, 2006.
[3] S.-S. Li, *et. al*., “Micromechanical “hollow-disk” ring...,” *MEMS'04*.
[4] L.-W. Hung, *et. al*., “Capacitive transducers…,” *Hilton Head,* 2008.
[5] T. J. Cheng and S. Bhave, “High-*Q*, low impedance polysilicon resonators with 10nm air gaps,” *MEMS'10*, pp. 695-698, 2010.
[6] S.-H. Lee, *et. al*., “Influence of electrode configurations on the quality factor…,” *J. Appl. Phys*, vol. 92, pp. 4062-4069, 2002.
[7] C.-L. Huang, *et. al*., “Effect of AlN film thickness and top electrode materials…,” *J. Appl. Phys*. vol. 44, pp. 1397-1402, 2005.
[8] M. Ueda, *et. al*., “High-*Q* resonators using FBAR/SAW technology…,” *Digest*, *IEEE Inter. Microwave Symp*., pp. 209-212, 2005.
[9] L. Mai, *et. al*., “ZnO-based film bulk acoustic resonator devices on a specially...,” *J. Applied Physics*, vol. 95, pp. 667-671, 2009.
[10] S. K. Kor, *et. al*., “Ultrasonic attenuation in pure and doped n-type silicon,” *J. Physical Review B*, vol. 10, pp. 775-778, 1974.
[11] D. K. Pandey, *et. al*., “Ultrasonic wave propagation in IIIrd group nitrides,” *Applied Acoustics*, vol. 68, pp. 766-777, 2007.
[12] R. Tabrizian, *et. al*, “Effect of phonon interactions on limiting the f*Q* product of micromechanical…,” *Transducers'09*, pp. 2131-2134.
[13] C. G. Courcimault and M. G. Allen, “High-*Q* mechanical tuning of MEMS resonators using a metal…,” *Transducers'05,* pp. 875-878.
[14] R. Besson, “A new ‘electrodeless’ resonator design,” *Freq. Control Symp*. pp. 147-152, 1976.
[15] C. Zuo, *et. al*., “1.05GHz MEMS oscillator based on lateral-field-excited piezoelectric…,” *Freq. Control Symp*, pp. 381-384, 2009.
[16] P. J. Stephanou and A. P. Pisano, "GHz higher order contour mode AlN annular resonators," *MEMS'07*, pp. 787-790.
[17] G. Piazza, *et. al*., "One and two port piezoelectric higher order contour-mode MEMS…," *Solid-State Electronics*, pp. 1596-1608, 2007.

CONTACT: Li-Wen Hung; lwhung@eecs.berkeley.edu